JOURNAL OF ENVIRONMENTAL SCIENCES 55 (2017) 331–338

Available online at www.sciencedirect.com

ScienceDirect

www.elsevier.com/locate/jes

JES JOURNAL OF ENVIRONMENTAL SCIENCES

www.jesc.ac.cn

# Template-free synthesis of inorganic hollow spheres at water/"water-brother" interfaces as Fenton-like reagents for water treatment

*Yingchun Su*[1], *Shenghua Ma*[1], *Xiaole Zhao*[1], *Mingdong Dong*[2], *Xiaojun Han*[1,*]

1. *MIIT Key Laboratory of Critical Materials Technology for New Energy Conversion and Storage, State Key Laboratory of Urban Water Resource and Environment, School of Chemistry and Chemical Engineering, Harbin Institute of Technology, Harbin 150001, China*
2. *Interdisciplinary Nanoscience Center, Aarhus University, Aarhus C DK-8000, Denmark*

ARTICLE INFO

*Article history:*
Received 3 July 2016
Revised 23 September 2016
Accepted 24 October 2016
Available online 18 November 2016

*Keywords:*
Inorganic hollow spheres
Water/"water-brother" interfaces
Watertreatment
Congo red
Fenton-like reaction

ABSTRACT

This paper reports a template-free method to synthesize a series of inorganic hollow spheres (IHSs) including Cu-1, Cu-2, Ni-1, Ni-2 based on mineralization reactions at water/"water-brother" interfaces. "Water-brother" was defined as a solvent which is miscible with water, such as ethanol and acetone. The water/"water-brother" interfaces are very different from water/oil interfaces. The "water-brother" solvent will usually form a homogenous phase with water. Interestingly, in our method, these interfaces can be formed, observed and utilized to synthesize hollow spheres. Utilizing the unique porous properties of the spheres, their potential application in water treatment was demonstrated by using Cu-1 IHSs as Fenton-like reagents for adsorption and decomposition of Congo Red from aqueous solution. The final adsorption equilibrium was achieved after 30 min with the maximum adsorption capacity of 86.1 mg/g, and 97.3% removal of the dye in 80 min after adsorption equilibrium. The IHSs can be reused as least 5 times after treatment by NaOH. This method is facile and suitable for large-scale production, and shows great potential for watertreatment.



## Introduction

Inorganic hollow spheres (IHSs) have attracted many scientists' attention due to their diverse applications such as catalysis (Chen et al., 2015; Zhu et al., 2013), energy storage (Li et al., 2013; Yang et al., 2013), supercapacitors (Cao et al., 2011; Ma et al., 2012), nanoreactors (Chen et al., 2010b; Fang et al., 2012), chemical sensors (Cheng et al., 2015; Li et al., 2015), watertreatment (Fei et al., 2008; Wang et al., 2012), and drug delivery (Su et al., 2015; Zhao et al., 2008). During the past several years, many methods have been developed to fabricate IHSs, using templates or template-free methods. The soft templates include emulsions (Guo et al., 2010), micelles (Sasidharan et al., 2011), vesicles (Xu and Wang, 2007), bubbles (Sun et al., 2013), and droplets (Jiang et al., 2004). Micelles of poly(styrene-b-acrylic acid-b-ethyleneoxide) and bubble templates were utilized to fabricate hollow titania nanospheres (Sasidharan et al., 2011) for rechargeable lithium-ion batteries and bismuth vanadate hollow spheres (Sun et al., 2013) for photocatalysis, respectively. The hard templates include latex cages (Yang et al., 2005), carbon spheres (Zhang et al., 2014), silica spheres (Chen et al., 2010a), hydrated metal sulfate spheres (Lu et al., 2011) and hematite spheres (Zhao et al., 2009) *etc.* For example, carbon

* *Corresponding author*. E-mail: hanxiaojun@hit.edu.cn (Xiaojun Han).

http://dx.doi.org/10.1016/j.jes.2016.10.012

spheres were used to prepare $Fe_3O_4$@$SiO_2$ hollow mesoporous spheres (Zhu et al., 2010) for drug delivery, and silica spheres were used as templates to synthesize hollow mesoporous aluminosilica spheres (Fang et al., 2012) for catalytic nanoreactors. Self-templating methods are a special case in hard-templating methods. The templates in self-templating methods (Fang et al., 2013; Ma et al., 2015) initially act as templates but gradually form the outer shells of the final IHSs. $Fe_3O_4$ hollow spheres (Ma et al., 2015) and hollow mesoporous silica (Fang et al., 2013) were synthesized using a self-templating strategy. Template-free methods have also been extensively used as an effective way to prepare hollow materials based on self-assembly (Mo et al., 2005; Zhou et al., 2015) and Ostwald ripening (Xu et al., 2014; Yec and Zeng, 2014). Hollow $ZnFe_2O_4$ microspheres (Zhou et al., 2015) were fabricated by self-assembly as acetone sensor. $Li_2FeSiO_4$ hollow spheres (Xu et al., 2014) as cathode materials for lithium-ion batteries were synthesized by Ostwald ripening.

Water is the most important and essential resource for life. Water pollution has become a serious issue all over the world. Some pollutants with high toxicity and carcinogenicity can seriously affect human health. Many metal oxide materials as potential adsorbents have been reported to effectively remove toxic heavy metal ions and organic pollutants from wastewater. These oxide materials include urchin-like α-FeOOH (Wang et al., 2012), hollow $SnO_2$ spheres (Shi and Lin, 2010), zeolite membranes (Kazemimoghadam, 2010), nanocrystalline copper/nickel oxide (Carnes et al., 2002), and 3D flowerlike ceria micro/nanocomposite (Zhong et al., 2007). Urchin-like α-FeOOH hollow spheres (Wang et al., 2012) were used for water treatment by absorption of As(V), Pb(II) and Congo Red. 3D flowerlike ceria micro/nanocomposites (Zhong et al., 2007) were used for removing As(V) and Cr(VI). Fenton/Fenton-like reactions are also common processes to deal with water pollution (Zbiljic et al., 2015). Through Fenton/Fenton-like reactions, many organic pollutants such as phenol (Babuponnusami and Muthukumar, 2012), aniline (Anotai et al., 2010), imidacloprid (Guzsvany et al., 2010), Methylene Blue (Dutta et al., 2001) and Congo Red (Zhang and Nan, 2014) can be oxidized by $Fe^{2+}$ (Wang, 2008), $Fe^{3+}$ (Chu et al., 2005) and $Cu^{2+}$ (Ruan et al., 2010). Fenton/Fenton-like reactions have also been used effectively in water treatment.

Herein we synthesized Cu-1 (Ni-1) and Cu-2 (Ni-2) IHSs using a crystallization – dissolution – interface mineralization (CDIM) method with water/"water-brother" (acetone, ethanol) interfaces respectively. A "water-brother" is a polar solvent which is miscible with water, such as acetone and ethanol. In the special method CDIM, water/"water-brother" interfaces can be formed, observed and utilized to synthesize IHSs. Cu-1 IHSs were proved to absorb and degrade Congo Red effectively, which gives these inorganic hollow spheres great potential in water treatment.

## 1. Materials and methods

### 1.1. Chemicals and reagents

Sodium hydroxide and hydrogen peroxide were purchased from Xilong Chemical (China). Cupric sulfate and nickel sulfate hexahydrate were purchased from Sinopharm Chemicals (China). Congo Red ($C_{32}H_{22}N_6Na_2O_6S_2$) was purchased from Tianjin Basifu Chemicals (China). Ethanol was purchased from Tianjin Tianli chemicals (China). Acetone was purchased from Tianjin Fuyu Fine Chemical (China). The solutions were prepared with ultrapure water (18.2 MΩ·$cm^{-1}$).

### 1.2. Preparation of IHSs

The crystal clusters of $CuSO_4$ and $NiSO_4$ were synthesized by injecting 250 μL saturated $CuSO_4$ (1.28 mol/L at 20°C) and $NiSO_4$ (1.79 mol/L at 20°C) aqueous solution into 25 mL acetone/ethanol under magnetic stirring (1400 r/min) for 3 hr. IHSs were formed by mixing together 1 mL crystals suspended in acetone/ethanol with a certain amount of NaOH water solution. The reaction lasted 3 min. The precipitates were washed by centrifuging with ultrapure water 3 times. Table 1 details the reactants, solvents, and amounts of NaOH used to prepare IHSs.

### 1.3. Observation of IHSs formation process under microscope

The processes for forming IHSs were observed by microscope. 25 μL crystal clusters in suspension and 25 μL or 50 μL of a certain concentration of NaOH solution were injected into a sealed cell in the proper order.

### 1.4. Adsorption and decomposition experiments for Congo Red

In absorption experiments, Congo Red (20 mL, 0.07 mg/mL), ultrapure water (19 mL) and Cu-1 IHSs (1 mL, 15.7 mg/mL) were mixed together. At certain time intervals, 3 mL of the mixture was taken out and centrifuged. The supernatant (2 mL) was measured by a UV–Vis spectrometer to calculate the concentration of Congo Red in solution according to the calibration curve shown in Appendix A Fig. S2. The adsorption kinetics curves were then obtained.

To optimize the concentration of $H_2O_2$, a mixture of Congo Red (1.5 mL, 0.14 mg/mL), ultrapure water (1.325 mL) and Cu-1 IHSs (75 μL, 15.7 mg/mL) was maintained for 40 min to reach absorption equilibrium. Then a certain concentration $H_2O_2$ (100 μL) was added into the mixture to obtain final concentrations of $H_2O_2$ of 0.16, 0.65, 1.13, 1.61, 3.22, 16.12 and 32.26 mmol/L. Similarly, 3 mL of the mixture was taken out after 80 min and centrifuged. The supernatant (2 mL) was measured by a UV–Vis spectrometer to calculate the concentration of Congo Red in solution to optimize the $H_2O_2$ concentration.

The following procedure was carried out to determine the dynamics of the Fenton-like reaction. A mixture of Congo Red

**Table 1 – The reactants, solvents and amounts of NaOH for IHSs (inorganic hollow spheres) synthesis.**

| | Reactant | "Water-brother" phase | Amount of NaOH |
|---|---|---|---|
| Cu-1 IHSs | $CuSO_4$ | Acetone | 2 mL 0.03 mol/L |
| Ni-1 IHSs | $NiSO_4$ | Acetone | 1 mL 0.13 mol/L |
| Cu-2 IHSs | $CuSO_4$ | Ethanol | 1 mL 0.06 mol/L |
| Ni-2 IHSs | $NiSO_4$ | Ethanol | 2 mL 0.15 mol/L |

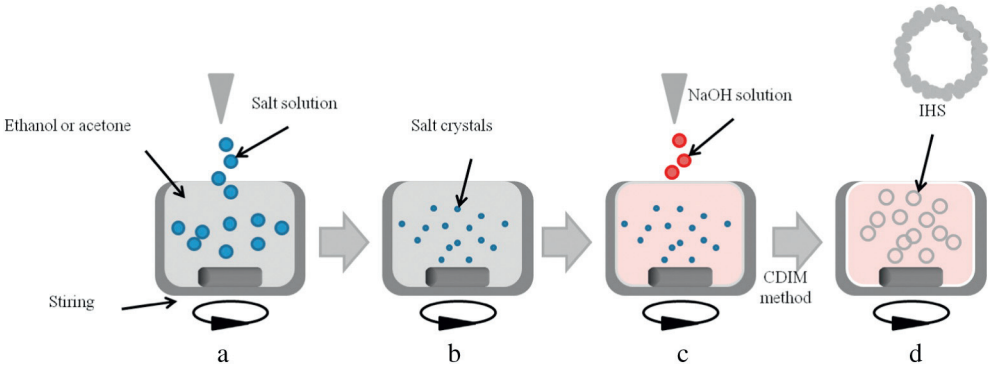


**Fig. 1 – Schematic of the IHSs formation progress. IHSs: inorganic hollow spheres.**

(20 mL, 0.14 mg/mL), ultrapure water (19 mL) and Cu-1 IHSs (1 mL, 15.7 mg/mL) was stirred for 40 min to reach absorption equilibrium. Afterwards $H_2O_2$ (64.4 μL, 1 mol/L) was added to the mixture. At certain time intervals, 3 mL of the mixture was taken out and centrifuged. The supernatants were measured using a UV–Vis spectrometer to obtain the concentration of Congo Red in solution, and consequently the curve of degradation efficiency against time was obtained.

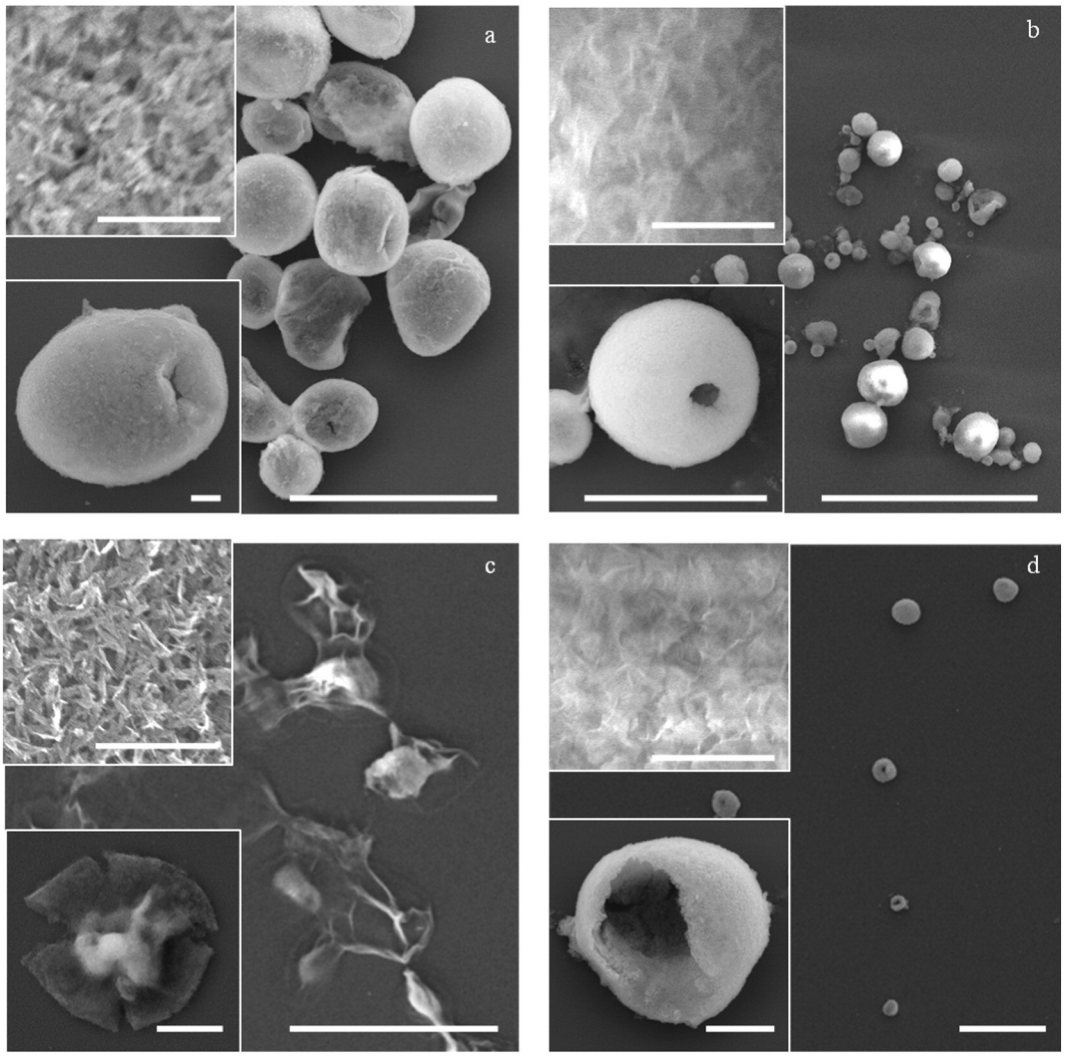


**Fig. 2 – SEM (scanning electron microscope) images of Cu-1(a), Ni-1(b), Cu-2(c) and Ni-2(d) IHSs. The scale bar is 50 μm. Insets (bottom left) in images are the enlarged images with the scale bar of 5 μm. Insets (top left) in images are the enlarged images at a higher magnification with the scale bar of 500 nm.**

To measure the stability of the Cu-1 IHSs, they were treated with 1 mol/L NaOH for 30 min and washed with ultrapure water three times before reuse.

### 1.5. *Characterization*

The morphologies of the Cu-1, Ni-1, Cu-2 and Ni-2 IHSs were characterized with a scanning electron microscope (Quanta 200 FEG, Netherlands) at an accelerating voltage of 20 kV. Silicon wafers were used as substrates. Powder X-ray diffraction (XRD) was measured in the reflection mode (Cu K radiation) on a diffractometer (D/Max-RB, Japan). Microscopic images were obtained using a Nikon Eclipse 80i fluorescence microscope. UV–Vis spectra were recorded using a Cary 60 UV–Vis spectrophotometer (Agilent, USA).

## 2. Results and discussion

Fig. 1 illustrates the method used to produce Cu and Ni spheres. The crystal clusters of $CuSO_4$/$NiSO_4$ were prepared by adding a certain amount of $CuSO_4$/$NiSO_4$ saturated solution into 25 mL ethanol/acetone (Fig. 1a). Due to the extraction of water by ethanol/acetone, $CuSO_4$/$NiSO_4$ were crystallized in the ethanol or acetone (Fig. 1b). Their XRD patterns, as shown in Appendix A Fig. S1, indicate the $CuSO_4$ crystallized in acetone to be a mixture of $CuSO_4$ and $CuSO_4{\cdot}3H_2O$ crystals according to standard data (PDF: 21-0269 and 22-0249), $NiSO_4$ crystals in acetone to be $NiSO_4{\cdot}6H_2O$ crystals according to standard data (PDF: 33-0955), $CuSO_4$ in ethanol to be $CuSO_4{\cdot}3H_2O$, and $NiSO_4$ in ethanol to be $NiSO_4{\cdot}6H_2O$ crystals, respectively. After crystallization, certain amounts of NaOH solution were added rapidly with stirring (Fig. 1c). The ethanol and acetone can be described as "water-brother" solvents due to their miscibility with water. When the NaOH solution is added, the water and "water-brother" are mixed together immediately. The salt crystal clusters can absorb the water from the "water-brother". As the water contacts them, the crystals are dissolved and form special interfaces with the "water-brother" solvent. At the water/"water-brother" interface, $Cu^{2+}$ and $Ni^{2+}$ ions meet with $OH^-$ and precipitate to form hollow spheres (Fig. 1d).

SEM (scanning electron microscope) images of these four IHSs (Fig. 2) show that the IHSs are spheres and the diameters of Cu-1, Ni-1, Cu-2 and Ni-2 spheres are 21, 5, 19 and 13 μm, respectively. The hollow structures are confirmed by the open hole in the zoomed-in image of a single sphere in the insets of Fig. 2a, b and d. The walls of Cu-2 IHSs are too thin to maintain their original shape in the vacuum chamber as shown in Fig. 2c, which also is proof of their hollow structure characteristic. By measuring the folded wrinkles, the wall thickness is shown to be 0.2 μm. On the contrary, the Cu-1, Ni-1 and Ni-2 IHSs are more rigid, with wall thicknesses of 1, 2 and

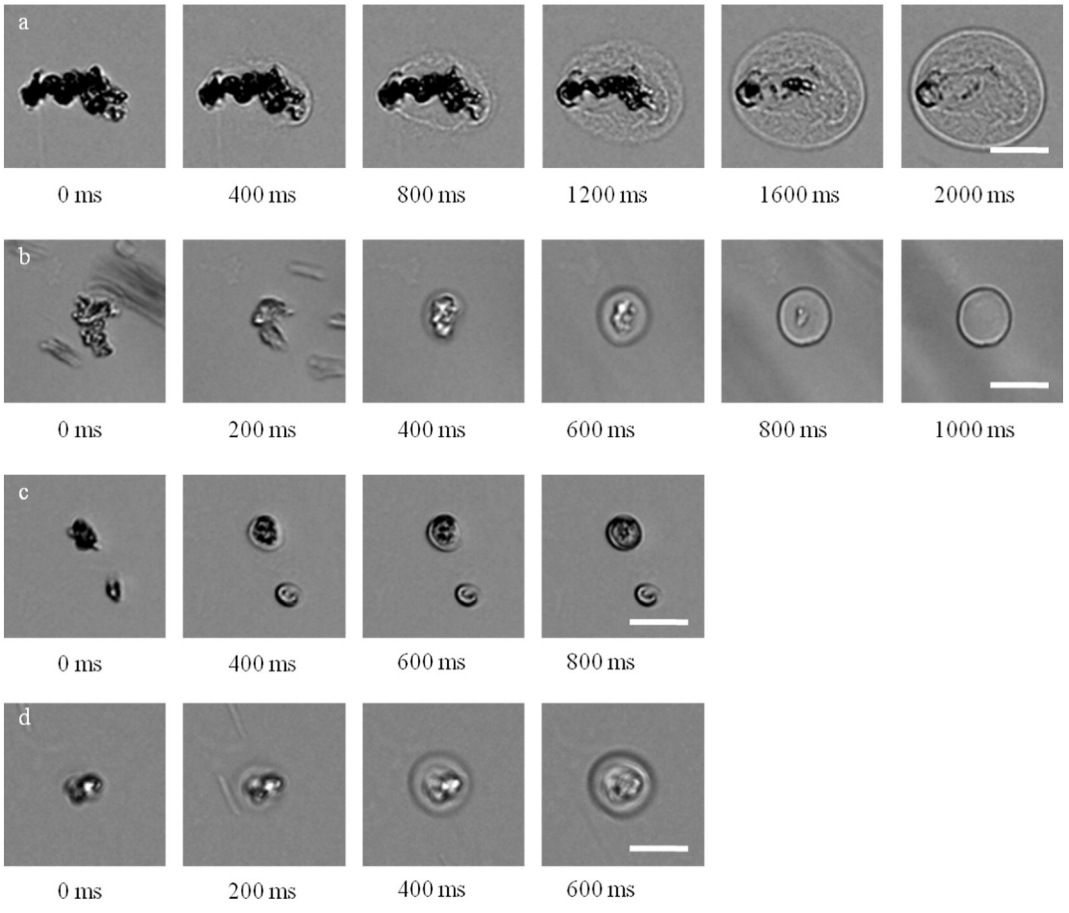


**Fig. 3 – The images of Cu-1(a), Ni-1(b), Cu-2(c) and Ni-2(d) IHS formation process. The scale bar is 20 μm.**

0.7 μm, respectively. As shown in the top insets of Fig. 2a and c, the shells are made of small particles and pores. The Cu-1 and Cu-2 IHSs have a porous structure, which is favorable for pollutant adsorption. The surfaces of Ni-1 and Ni-2 spheres are rough. The XRD patterns of Cu-1, Ni-1, Cu-2 and Ni-2 are shown in Appendix A Fig. S1e, f, g and h, and show that the Cu-1 samples are $Cu(OH)_2$ (PDF:13-0420), Cu-2 are mixtures of $Cu_4SO_4(OH)_6{\cdot}2H_2O$ and CuO according to PDF: 43-0670 and 45-0937, and the Ni-1 and Ni-2 samples are amorphous without sharp peaks.

The formation processes of Cu and Ni IHSs were captured with a bright field microscope, as shown in Fig. 3. The transformations of crystals to IHSs are clearly presented. The formation time of Cu-1, Ni-1, Cu-2 and Ni-2 are 2, 1, 0.8 and 0.6sec, respectively. The crystal clusters gradually disappeared whilst the diameter of interface circles increased. The water/"water-brother" interfaces can be observed clearly. The precipitation at the interfaces took place to form microspheres.

Porous materials are often utilized for water treatment because of their capability to adsorb and oxidize a large quantity of pollutants including both organic (Chen et al., 2013; Tan et al., 2008) and inorganic (Zhong et al., 2007) substances. For the purpose of environmental protection, we investigated the application of Cu-1 IHSs in water treatment for removal of Congo Red, which is a dye used commonly in the textile industry. Fig. 4a shows the adsorption capacity of Cu-1 IHSs towards Congo Red at room temperature. It can be seen that the adsorption is very fast at the beginning stage, and then it becomes slower and finally reaches equilibrium. The adsorption data were obtained based on the calibration curve of Congo Red (Appendix A Fig. S2). From the spectra and the inset photograph, it can be seen that the Congo Red can be completely removed from the water. In order to illustrate the dye adsorption rate, the adsorption kinetic curve of Cu-1 IHSs for Congo Red is shown in Fig. 4b. The pseudosecond-order kinetic rate model (Ho and McKay, 1998) (Eq. (1)) was used to fit the experimental results obtaining a correlation coefficient $R^2$ of 0.9998. Fig. 4c shows the adsorption spectra of Congo Red solutions after being treated for different times by 15.7 mg of Cu-1 IHSs. The pure

**Table 2 – Comparison of the adsorption capacity of Congo Red onto various adsorbents.**

| Adsorbents | Maximum adsorption capacity (mg/g) | References |
|---|---|---|
| Cu-1 IHSs | 86.1 | Our work |
| Zeolites | 69.94 | Liu et al. (2014) |
| Ca-bentonite | 85.29 | Lian et al. (2009) |
| Anilinepropylsilica xerogel | 22.62 | Pavan et al. (2008) |
| Hollow Zn-$Fe_2O_4$ nanospheres | 16.58 | Rahimi et al. (2011) |

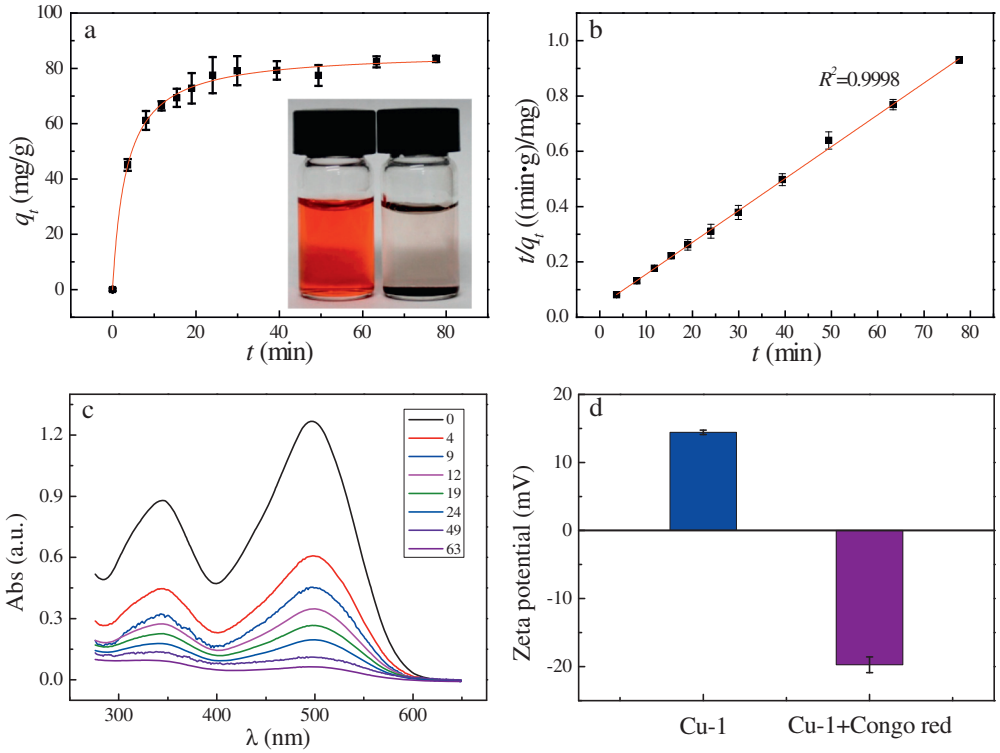


**Fig. 4 – (a) Adsorption kinetics of Cu-1 IHSs for Congo Red. The inset shows the photograph of the same concentration of Congo Red before (left) and after (right) adding Cu-1 IHSs; (b) The pseudo-second-order plot transformed from curve in (a); (c) UV–Vis adsorption spectra of Congo Red solutions after being treated with 15.7 mg Cu-1 IHSs at 0, 4, 9, 12, 19, 24, 49 and 63 min, respectively. (d) The values of zeta potential for pure Cu-1 and Cu-1 with absorbed Congo Red.**

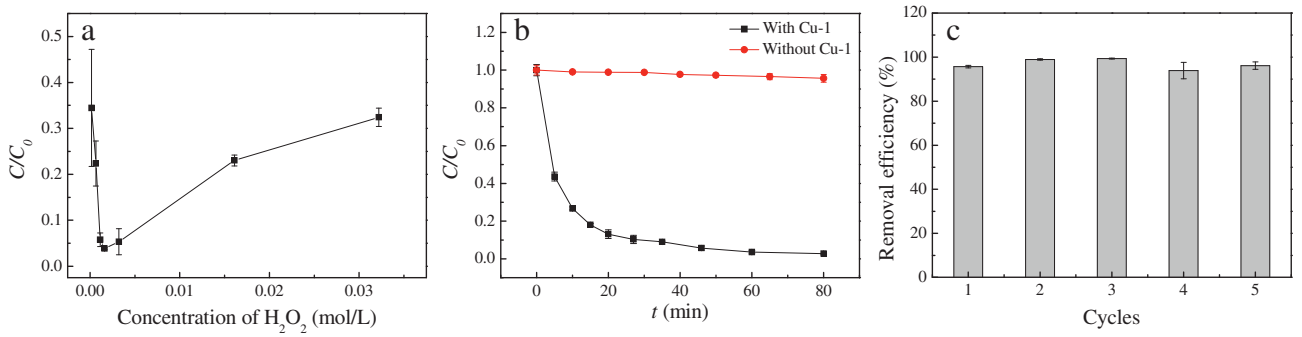


**Fig. 5 – (a) The effect of $H_2O_2$ concentration on the degradation efficiency of 70 mg/L Congo Red with 392.5 mg/L Cu-1 IHSs in 1 hr; (b) The degradation efficiency against time with and without Cu-1 IHSs. (c) Stability of Cu-1 IHSs in the degradation of 70 mg/L Congo Red.**

Cu-1 IHSs are positively charged due to their zeta potential of 14.4 mV, as shown in Fig. 4d, which is favorable for adsorbing the negatively charged Congo Red molecules. After adsorption, the zeta potential of Cu-1 IHSs shifted from 14.4 to −19.7 mV. Table 2 lists a comparison of the adsorption capacities of various adsorbents towards Congo Red. From Table 2, it is noted that the Cu-1 IHSs prepared in this work have an adsorption capacity of 86.1 mg/g, which is relatively large compared with the other materials.

$$t/q_t = 1/kq_e^{\,2} + t/q_e \quad (1)$$

where, $k$ is the rate constant, and $q_t$ (mg/g) and $q_e$ (mg/g) are the amount of dye sorbed at time $t$ (min) and equilibrium state, respectively.

Fig. 5a shows the effect of $H_2O_2$ concentration on the degradation efficiency of 392.5 mg/L Cu-1 IHSs towards 70 mg/L Congo Red in a 1 hr reaction. From 0.16 to 1.61 mmol/L the degradation efficiency (Eq. (2)) of the dye increased from 65.6% to 96.1%, and from 1.61 to 32.26 mmol/L the degradation efficiency decreased to 67.7%. Thus 1.61 mmol/L is the best condition for oxidation, which was adopted in subsequent experiments. Fig. 5b shows a comparison of the dye degradation efficiency with and without Cu-1 IHS catalysts. The extent of dye degradation was 97.3% with Cu-1 IHSs and 4.3% without Cu-1 IHSs after 80 min. The catalysts thus have a positive effect on the Fenton-like reaction. As shown in Fig. 5c, the Cu-1 IHSs catalyst can be reused at least five times, showing the degradation efficiencies for Congo Red of 95.7%, 99.0%, 99.4%, 93.9% and 96.1%, respectively. Surprisingly, the second and third cycles showed better results, which may due to residual $OH^-$ on Cu-1 IHSs. In Appendix A Fig. S3, the effect of NaOH concentration was investigated. Trace amounts of NaOH can increase the dye degradation efficiency (from 0 to 16 μmol/L). In the fourth and fifth cycles, the decrease of degradation efficiency may be due to the loss of Cu-1 IHSs in the recycling step.

$$\text{Degration efficiency} = (1-C/C_0) \times 100\% \quad (2)$$

where C (mg/L) and $C_0$ (mg/L) are the amount of dye in solution at time t and equilibrium state, respectively.

The positive zeta potential of Cu-1 IHSs was due to the adsorption of $Cu^{2+}$ ions at the surface. The $Cu^{2+}$ ions on Cu-1 IHSs were the active sites for the Fenton-like reaction. The reaction mechanism (Xiao et al., 2013) was proposed as shown below (Eqs. (3)–(5)):

$$Cu^{2+}-(Cu-1IHSs) + H_2O_2 \rightarrow \bullet OOH + Cu^{+}-(Cu-1IHSs) + H^{+} \quad (3)$$

$$Cu^{+}-(Cu-1IHSs) + H_2O_2 \rightarrow Cu^{2+}-(Cu-1IHSs) + \bullet OH + OH^{-} \quad (4)$$

$$\bullet OH + \text{Congo Red} \rightarrow \text{oxidation products} \quad (5)$$

## 3. Conclusions

Water/“water-brother” interfaces in the CDIM method were used to prepare Cu-1, Ni-1, Cu-2 and Ni-2 inorganic hollow spheres. The water/“water-brother” interfaces were observed by microscope. The morphology, formation process and crystal structures of these IHSs were investigated with SEM, microscopy, and XRD respectively. They were formed very quickly, within a few seconds.

## Acknowledgments

This work was supported by the National Natural Science Foundation of China (Nos. 21273059, 21528501, 21511130060), and the HIT Environment and Ecology Innovation Special Funds (No. HSCJ201617).

## Appendix A. Supplementary data

Supplementary data to this article can be found online at http://dx.doi.org/10.1016/j.jes.2016.10.012.

## REFERENCES

Anotai, J., Su, C.C., Tsai, Y.C., Lu, M.C., 2010. Effect of hydrogen peroxide on aniline oxidation by electro-Fenton and fluidized-bed Fenton processes. J. Hazard. Mater. 183 (1–3), 888–893.

Babuponnusami, A., Muthukumar, K., 2012. Advanced oxidation of phenol: a comparison between Fenton, electro-Fenton, sono-electro-Fenton and photo-electro-Fenton processes. Chem. Eng. J. 183, 1–9.

Cao, C.Y., Guo, W., Cui, Z.M., Song, W.G., Cai, W., 2011. Microwave-assisted gas/liquid interfacial synthesis of flowerlike NiO hollow nanosphere precursors and their application as supercapacitor electrodes. J. Mater. Chem. 21 (9), 3204–3209.

Carnes, C.L., Stipp, J., Klabunde, K.J., 2002. Synthesis, characterization, and adsorption studies of nanocrystalline copper oxide and nickel oxide. Langmuir 18 (4), 1352–1359.

Chen, Y., Chen, H.R., Guo, L.M., He, Q.J., Chen, F., Zhou, J., Feng, J.W., Shi, J.L., 2010a. Hollow/rattle-type mesoporous nanostructures by a structural difference-based selective etching strategy. ACS Nano 4 (1), 529–539.

Chen, Z., Cui, Z.M., Niu, F., Jiang, L., Song, W.G., 2010b. Pd nanoparticles in silica hollow spheres with mesoporous walls: a nanoreactor with extremely high activity. Chem. Commun. 46 (35), 6524–6526.

Chen, R.X., Yu, J.G., Xiao, W., 2013. Hierarchically porous $MnO_2$ microspheres with enhanced adsorption performance. J. Mater. Chem. A 1 (38), 11682–11690.

Chen, J., Wang, D.W., Qi, J., Li, G.D., Zheng, F.Y., Li, S.X., Zhao, H.J., Tang, Z.Y., 2015. Monodisperse hollow spheres with sandwich Heterostructured shells as high-performance catalysts via an extended $SiO_2$ template method. Small 11 (4), 420–425.

Cheng, C.M., Huang, Y., Wang, N., Jiang, T., Hu, S., Zheng, B.Z., Yuan, H.Y., Xiao, D., 2015. Facile fabrication of $Mn_2O_3$ nanoparticle-assembled hierarchical hollow spheres and their sensing for hydrogen peroxide. ACS Appl. Mater. Interfaces 7 (18), 9526–9533.

Chu, W., Kwan, C.Y., Chan, K.H., Kam, S.K., 2005. A study of kinetic modelling and reaction pathway of 2,4-dichlorophenol transformation by photo-Fenton-like oxidation. J. Hazard. Mater. 121 (1), 119–126.

Dutta, K., Mukhopadhyay, S., Bhattacharjee, S., Chaudhuri, B., 2001. Chemical oxidation of methylene blue using a Fenton-like reaction. J. Hazard. Mater. 84 (1), 57–71.

Fang, X.L., Liu, Z.H., Hsieh, M.F., Chen, M., Liu, P.X., Chen, C., Zheng, N.F., 2012. Hollow mesoporous aluminosilica spheres with perpendicular pore channels as catalytic nanoreactors. ACS Nano 6 (5), 4434–4444.

Fang, X.L., Zhao, X.J., Fang, W.J., Chen, C., Zheng, N.F., 2013. Self-templating synthesis of hollow mesoporous silica and their applications in catalysis and drug delivery. Nanoscale 5 (6), 2205–2218.

Fei, J.B., Cui, Y., Yan, X.H., Qi, W., Yang, Y., Wang, K.W., He, Q., Li, J.B., 2008. Controlled preparation of $MnO_2$ hierarchical hollow nanostructures and their application in water treatment. Adv. Mater. 20 (3), 452–456.

Guo, P., Song, H.H., Chen, X.H., 2010. Hollow graphene oxide spheres self-assembled by W/O emulsion. J. Mater. Chem. 20 (23), 4867–4874.

Guzsvany, V., Banic, N., Papp, Z., Gaal, F., Abramovic, B., 2010. Comparison of different iron-based catalysts for photocatalytic removal of imidacloprid. React. Kinet. Mech. Catal. 99 (1), 225–233.

Ho, Y.S., McKay, G., 1998. Sorption of dye from aqueous solution by peat. Chem. Eng. J. 70 (2), 115–124.

Jiang, Z.Y., Xie, Z.X., Zhang, X.H., Lin, S.C., Xu, T., Xie, S.Y., Huang, R.B., Zheng, L.S., 2004. Synthesis of single-crystalline ZnO polyhedral submicrometer-sized hollow beads using laser-assisted growth with ethanol droplets as soft templates. Adv. Mater. 16 (11), 904–907.

Kazemimoghadam, M., 2010. New nanopore zeolite membranes for water treatment. Desalination 251 (1), 176–180.

Li, D., Qin, Q., Duan, X.C., Yang, J.Q., Guo, W., Zheng, W.J., 2013. General one-pot template-free hydrothermal method to metal oxide hollow spheres and their photocatalytic activities and lithium storage properties. ACS Appl. Mater. Interfaces 5 (18), 9095–9100.

Li, J.W., Liu, X., Cui, J.S., Sun, J.B., 2015. Hydrothermal synthesis of self-assembled hierarchical tungsten oxides hollow spheres and their gas sensing properties. ACS Appl. Mater. Interfaces 7 (19), 10108–10114.

Lian, L.L., Guo, L.P., Guo, C.J., 2009. Adsorption of Congo red from aqueous solutions onto Ca-bentonite. J. Hazard. Mater. 161 (1), 126–131.

Liu, S.G., Ding, Y.Q., Li, P.F., Diao, K.S., Tan, X.C., Lei, F.H., Zhan, Y.H., Li, Q.M., Huang, B., Huang, Z.Y., 2014. Adsorption of the anionic dye Congo red from aqueous solution onto natural zeolites modified with N,N-dimethyl dehydroabietylamine oxide. Chem. Eng. J. 248, 135–144.

Lu, X.J., Huang, F.Q., Wu, J.J., Ding, S.J., Xu, F.F., 2011. Intelligent hydrated-sulfate template assisted preparation of nanoporous $TiO_2$ spheres and their visible-light application. ACS Appl. Mater. Interfaces 3 (2), 566–572.

Ma, F.W., Zhao, H., Sun, L.P., Li, Q., Huo, L.H., Xia, T., Gao, S., Pang, G.S., Shi, Z., Feng, S.H., 2012. A facile route for nitrogen-doped hollow graphitic carbon spheres with superior performance in supercapacitors. J. Mater. Chem. 22 (27), 13464–13468.

Ma, F.X., Hu, H., Wu, H.B., Xu, C.Y., Xu, Z.C., Zhen, L., Lou, X.W., 2015. Formation of uniform $Fe_3O_4$ hollow spheres organized by ultrathin nanosheets and their excellent lithium storage properties. Adv. Mater. 27 (27), 4097–4101.

Mo, M.S., Yu, J.C., Zhang, L.Z., Li, S.K., 2005. Self-assembly of ZnO nanorods and nanosheets into hollow microhemispheres and microspheres. Adv. Mater. 17 (6), 756–760.

Pavan, F.A., Dias, S.L.P., Lima, E.C., Benvenutti, E.V., 2008. Removal of Congo red from aqueous solution by anilinepropylsilica xerogel. Dyes Pigments 76 (1), 64–69.

Rahimi, R., Kerdari, H., Rabbani, M., Shafiee, M., 2011. Synthesis, characterization and adsorbing properties of hollow Zn-$Fe_2O_4$ nanospheres on removal of Congo red from aqueous solution. Desalination 280 (1), 412–418.

Ruan, Y.B., Li, C., Tang, J., Xie, J., 2010. Highly sensitive naked-eye and fluorescence "turn-on" detection of $Cu^{2+}$ using Fenton reaction assisted signal amplification. Chem. Commun. 46 (48), 9220–9222.

Sasidharan, M., Nakashima, K., Gunawardhana, N., Yokoi, T., Inoue, M., Yusa, S., Yoshio, M., Tatsumi, T., 2011. Novel titania hollow nanospheres of size 28 ± 1 nm using soft-templates and their application for lithium-ion rechargeable batteries. Chem. Commun. 47 (24), 6921–6923.

Shi, L.A., Lin, H.L., 2010. Facile fabrication and optical property of hollow $SnO_2$ spheres and their application in water treatment. Langmuir 26 (24), 18718–18722.

Su, Y.C., Zong, W., Zhao, X.L., Ma, S.H., Han, X.J., 2015. Inorganic microcapsules mineralized at the interface of water droplets in ethanol solution and their application as drug carriers. RSC Adv. 5 (100), 82247–82251.

Sun, J.X., Chen, G., Wu, J.Z., Dong, H.J., Xiong, G.H., 2013. Bismuth vanadate hollow spheres: bubble template synthesis and enhanced photocatalytic properties for photodegradation. Appl. Catal. B Environ. 132, 304–314.

Tan, I.A.W., Ahmad, A.L., Hameed, B.H., 2008. Adsorption of basic dye on high-surface-area activated carbon prepared from coconut husk: equilibrium, kinetic and thermodynamic studies. J. Hazard. Mater. 154 (1), 337–346.

Wang, S.B., 2008. A comparative study of Fenton and Fenton-like reaction kinetics in decolourisation of wastewater. Dyes Pigments 76 (3), 714–720.

Wang, B., Wu, H.B., Yu, L., Xu, R., Lim, T.T., Lou, X.W., 2012. Template-free formation of uniform urchin-like α-FeOOH

hollow spheres with superior capability for water treatment. Adv. Mater. 24 (8), 1111–1116.
Xiao, S.L., Liu, Y.G., Qin, L., Cui, G.H., 2013. A hexanuclear Cu II-based coordination framework with non-interpenetrated α-Po topology displaying catalytic activity. Inorg. Chem. Commun. 36, 220–223.
Xu, H.L., Wang, W.Z., 2007. Template synthesis of multishelled $Cu_2O$ hollow spheres with a single-crystalline shell wall. Angew. Chem. Int. Ed. 46 (9), 1489–1492.
Xu, Y.M., Shen, W., Zhang, A.L., Liu, H.M., Ma, Z.F., 2014. Template-free hydrothermal synthesis of $Li_2FeSiO_4$ hollow spheres as cathode materials for lithium-ion batteries. J. Mater. Chem. A 2 (32), 12982–12990.
Yang, M., Ma, J., Niu, Z.W., Dong, X., Xu, H.F., Meng, Z.K., Jin, Z.G., Lu, Y.F., Hu, Z.B., Yang, Z.Z., 2005. Synthesis of spheres with complex structures using hollow latex cages as templates. Adv. Funct. Mater. 15 (9), 1523–1528.
Yang, S.L., Hu, M.J., Xi, L.J., Ma, R.G., Dong, Y.C., Chung, C.Y., 2013. Solvothermal synthesis of monodisperse $LiFePO_4$ micro hollow spheres as high performance cathode material for lithium ion batteries. ACS Appl. Mater. Interfaces 5 (18), 8961–8967.
Yec, C.C., Zeng, H.C., 2014. Synthesis of complex nanomaterials via Ostwald ripening. J. Mater. Chem. A 2 (14), 4843–4851.
Zbiljic, J., Vajdle, O., Guzsvany, V., Molnar, J., Agbaba, J., Dalmacija, B., Kalcher, K., 2015. Hydrodynamic chronoamperometric method for the determination of $H_2O_2$ using $MnO_2$-based carbon paste electrodes in groundwater treated by Fenton and Fenton-like reagents for natural organic matter removal. J. Hazard. Mater. 283, 292–301.
Zhang, T., Nan, Z.R., 2014. Decolorization of methylene blue and Congo red by attapulgite-based heterogeneous Fenton catalyst. Desalin. Water Treat. 57 (10), 4633–4640.
Zhang, G.Q., Wu, H.B., Song, T., Paik, U., Lou, X.W., 2014. $TiO_2$ hollow spheres composed of highly crystalline nanocrystals exhibit superior lithium storage properties. Angew. Chem. Int. Ed. 53 (46), 12590–12593.
Zhao, W.R., Chen, H.R., Li, Y.S., Li, L., Lang, M.D., Shi, J.L., 2008. Uniform rattle-type hollow magnetic mesoporous spheres as drug delivery carriers and their sustained-release property. Adv. Funct. Mater. 18 (18), 2780–2788.
Zhao, W.R., Lang, M.D., Li, Y.S., Li, L., Shi, J.L., 2009. Fabrication of uniform hollow mesoporous silica spheres and ellipsoids of tunable size through a facile hard-templating route. J. Mater. Chem. 19 (18), 2778–2783.
Zhong, L.S., Hu, J.S., Cao, A.M., Liu, Q., Song, W.G., Wan, L.J., 2007. 3D flowerlike ceria micro/nanocomposite structure and its application for water treatment and CO removal. Chem. Mater. 19 (7), 1648–1655.
Zhou, X., Li, X.W., Sun, H.B., Sun, P., Liang, X.S., Liu, F.M., Hu, X.L., Lu, G.Y., 2015. Nanosheet-assembled $ZnFe_2O_4$ hollow microspheres for high-sensitive acetone sensor. ACS Appl. Mater. Interfaces 7 (28), 15414–15421.
Zhu, Y.F., Ikoma, T., Hanagata, N., Kaskel, S., 2010. Rattle-type $Fe_3O_4$@$SiO_2$ hollow mesoporous spheres as carriers for drug delivery. Small 6 (3), 471–478.
Zhu, L.P., Wang, L.L., Bing, N.C., Huang, C., Wang, L.J., Liao, G.H., 2013. Porous fluorine-doped gamma-$Fe_2O_3$ hollow spheres: synthesis, growth mechanism, and their application in photocatalysis. ACS Appl. Mater. Interfaces 5 (23), 12478–12487.